Fabrication and Study of $LaNi_{0.6}Fe_{0.4}O_{3-\delta}$ and $Sm_{0.5}Sr_{0.5}CoO_{3-\delta}$ Composite Cathode

Zetian Tao (taozetian@usc.edu.cn)
University of South China https://orcid.org/0000-0002-5169-989X
Yong Liu
University of South China
Min Fu
University of South China
Hailu Dai
Yancheng Institute of Technology

Rapid Communication

Keywords: Solid oxide fuel cells, Composite cathode, Catalytic activity, electrochemical performance

Posted Date: April 3rd, 2021

DOI: https://doi.org/10.21203/rs.3.rs-376930/v1

Abstract

In this paper, the composite cathode material of of $LaNi_{0.6}Fe_{0.4}O_{3-\delta}$(LNF) and $Sm_{0.5}Sr_{0.5}CoO_{3-\delta}$(SSC) is investigated and the cell performance of $BaCe_{0.7}Y_{0.2}Zr_{0.1}O_{3-\delta}$(BZCY)-based proton-conducting solid oxide fuel cell (H-SOFC) is evaluated. LNF powders and SSC powders with different ratios (1:0, 7:3, 5:5, 3:7, 0:1 wt. %) are mixed as the composite cathode to explore the optimized composition. The phase structure of the fabricated cathode powders is analyzed through X-ray diffraction method (XRD) and no second phase was observed below 1000^oC, showing good chemical compatibility. The electrochemical properties consisted of I-V and EIS curves reveal that the single cell with LNF-SSC73 cathode has the best electrochemical performance, exhibiting a polarization resistance of 0.10 $\Omega \cdot cm^2$ and a relatively high maximum power density of 636 $mWcm^2$ at 700^oC. These results above indicate that LNF-SSC73 composite material could improve the performance of fuel cells, which would be a prospective material in the field of H-SOFC.

Introduction

Proton solid oxide fuel cells (H-SOFCs) has been attracting much attention over the past decades for its lower ion conduction activation energy and higher cell conversion efficiency than traditional oxygen ion SOFC, making it easy for protons to pass through the dense electrolyte layer to the cathode at intermediate temperature [1-3]. In addition, it doesn't lead to dilution of H_2 as water is produced on the cathode side in H-SOFC[4].

$BaCe_{0.7}Zr_{0.1}Y_{0.2}O_3$ (BZCY) which is perceived as one of ideal electrolytes for H-SOFC, is of significant importance for its elevated stability and superior bulk proton conductivity [5]. Nevertheless, increasing the rate-limiting step of cathode reaction such as oxygen reduction reaction and oxygen ion diffusion is still undoubtedly deemed as a great challenge[6]. Proper cathode materials with mixed electron and ion conductivity, such as $La_xSr_{1-x}Co_yFe_{1-y}O_{3-\delta}$(LSCF)[7]$Sm_{0.5}Sr_{0.5}CoO_{3-\delta}$(SSC)[8] and $Ba_{0.5}Sr_{0.5}Co_{0.8}Fe_{0.2}O_{3-\delta}$(BSCF)[9] have been reported and the electrochemical performances are evaluated [10-12]. Notably, these cathodes normally encounter problems such as high thermal expansion coefficients (TEC) attributable to the high cobalt content at the B sites in the perovskite structure. Thus, it may be crucial to develop novel cathode materials with good thermal expansion compatibility and excellent performance during actual fuel cell application. As a Co-free cathode material, $LaNi_{0.6}Fe_{0.4}O_{3-\delta}$ (LNF) has high electrical conductivity at low temperature, good thermal and chemical stability [13-15]. In contrast with SSC material, the oxygen catalytic activity of this kind of materials is relatively weak, making the performance need to be highly improved[16]. Therefore, considering the different properties of the two types of cathode materials, we try to explore the possibility of the composite cathode mixing with LNF and SSC as a part of the SOFC system at intermediate temperature in this study.

Moreover, as mentioned in previous study, the proton-blocking composite cathode exhibits a higher cell performance than traditional proton-conducting composite cathode [16-18]. The detrimental effect on the

oxidant and electrochemical reaction sites in the cathode caused by high water vapor partial pressure can be limited by using the proton-blocking cathode. The composite cathode of LNF and SSC with mainly oxygen ion conductivity and electron conductivity also present proton-blocking feature as per its interstitial mechanism and still there are no reports about this composite material. Thus, considering the advantages presented above, the composite cathode of LNF and SSC with different ratio were firstly prepared and the electrochemical performance was evaluated to observe the potential for BZCY based H-SOFC.

Experimental

Materials synthesis

LNF□SSC and BZCY powders were synthesized through a conventional combustion method with citric acid as the combustion agent [3, 19, 20]. The raw materials used for LNF powders were La_2O_3, $Ni(NO_3)_2{\cdot}6H_2O$ and $Fe(NO_3)_3{\cdot}9H_2O$ and Sm_2O_3, $SrCO_3$ and $Co(NO_3)_2{\cdot}H_2O$ were used for synthesize SSC, while $BaCO_3$, $Zr(NO_3)_4{\cdot}5H_2O$, $Ce(NO_3)_3{\cdot}6H_2O$ and $Y(NO_3)_3{\cdot}6H_2O$ served as the raw materials for BZCY powders. All the raw materials were bought from Aladdin Corporation and the detailed synthesize process can been found in our previous studies[21].

Cell preparation

The anode substrate consisted of BZCY□NiO and starches at a weight ratio of 40:60:20 were firstly pressed under 250 MPa. Then, half-cell was prepared through co-pressing loose BZCY powders on the anode substrate through a co-pressing method at 300MPa and subsequently sintered at 1350 °C for 5 h. LNF powders and SSC powders are mixed with different ratios (1:0, 7:3, 5:5, 0:1 wt.%) as the composite cathode, which were named as LNF-SSC10, LNF-SSC73, LNF-SSC55 and LNF-SSC01, respectively. The mixtures were deposited on the electrolyte layer using screen-printing method and co-fired at 1000 °C for 3 h.

Characterizations

To identify the crystal phase and structure parameters of prepared LNF, SSC and LNF-SSC mixture powders, X-ray diffraction (XRD, X'Pert3Powder) was employed using CuKa radiation. Meanwhile, cell morphology was characterized by scanning electron microscopes (SEM, Nova NanoSEM 450). The single cell performance was evaluated using a Zahner Zennium electrochemical workstation at temperatures from 600 to 700^oC using wet (3%H_2O) H_2 as fuel and ambient air as oxidant

Results And Discussion

For the composite cathode of LNF and SSC, the chemical compatibility between the two components should be taken into consideration first. The cell performance based on the cathode will be influenced due to the impurity formation which may be insulated or low electrochemical activity. Fig. 1 shows XRD

patterns of synthesized LNF-SSC55 calcined at the temperatures from 900^{o}C to 1150^{o}C for 3 h. One can see that only peaks corresponding to LNF and SSC can be found and there are no obvious impurities, suggesting LNF is chemically compatible with SSC up to 1000^{o}C. In other words, there is no chemical reaction between LNF powder and SSC powder with no impurity phase is generated. When the temperature increased to 1100^{o}C, the diffraction pattern of LNF-SSC55 showed an additional diffraction peak at a diffraction angle of about 44°, which may be due to a certain chemical reaction between LNF and SSC at 1100^{o}C. In sum, we can conclude that LNF and SSC will not reacts and forms impurities at 1000^{o}C, indicating that the intrinsic electrochemical catalytic activity will not be influenced and the temperature is suitable to assemble cathode layer.

The microstructures of the cells with different composite cathodes were investigated by SEM and shown In Figure 2 and Figure 3. As shown in figure 2, it can be observed that all the cathodes are porous with certain porosity to ensure the transmission of oxygen. Meanwhile, LNF particle size is smaller than SSC particle size, and the particle size of cathode increases gradually with the increase content of SSC. Though LNF particles have higher specific area, the poor ion-conductivity and catalytic ability limit the length of triple phase boundary which is crucial to the adsorption and dissociation rate of ambient oxygen on the electrode boundary [22]. In Fig. 3, the cross-sectional morphology of single cells with all cathodes can be clearly observed and no obvious cracks and spelling phenomenon are found, indicating that the composite cathode was in good contact with the electrolyte and the cathode firing temperature used 1000^{o}C is appropriate. Moreover, the BZCY electrolyte layer is very dense without any obvious pores inside, suggesting the sintering temperature is adequate to avoid gas leakage through the electrolyte.

Figure 4 and 5 showed the I–V and power density curves for the cell with LNF-SSC composite cathodes and a comparison of impedance plots of fuel cells using LNF-SSC composite cathodes measured at 700 °C. One can see that LNF-SSC73 shows the best cell performance with maximum power density (MPDs) reaching 636mW·cm^{-2} and the polarization resistance (Rp) reaching 0.10Ω·cm^{2}. As can be seen from the figure, the Rp value of LNF-SSC73 composite cathode was much lower than that of LNF and SSC single-phase cathode which is about 0.34 and 0.18Ω·cm^{2}, respectively. These single cells are prepared by the same method, and the thickness of the BZCY layer is almost the same, so the significant improvement of cell performance comes from the cathode. This may be due to its higher electrochemical activity and conductivity, which is more conducive to the generation and transmission of O^{2-}.

In addition, the electrochemical performance of cell with cathode LNF-SSC73 at elevated temperature from 600-700^{o}C is tested under the cell operation conditions. As shown in figure 6, the MPDs of 636, 437, 300mW cm^{-2} with the OCV values of 0.978, 1.003 and 1.028V are gained at 700, 650 and 600 ˚C for the single cell, respectively. Meanwhile, electrochemical impedance spectra under open circuit conditions is tested at various temperatures and shown in Figure 7 to further investigate the influcence of temperatures on the polarization resistances of the cathode. As can be seen in figure 7, the overall ohm resistance has a negative relationship with the temperature, reducing from 0.71 Ω cm^{2} at 600 ˚C to 0.28 Ω cm^{2} at 700 ˚C. Furthermore, it is obviously that the Rp is significantly determined by the operation temperatures,

decreasing typically from 0.41 Ω cm^2 at 600 ˚C to 0.10 Ω cm^2 at 700 ˚C. As shown in figure, two obvious arcs are observed in the impedance spectrum, which means that there are at least two rate limiting steps related to the oxygen ion transfer and oxygen adsorption-dissociation processes.

In order to deeply study the influence of the polarization resistances, distribution of relaxation time (DRT) method is applied to identify the polarization processes using the impedance spectra tested under OCV conditions[23, 24]. As shown in figure 8, there are four main peaks existed in the curve F (τ) vs. τ (relaxation time) named as P3、P2、Padd2 and P1, respectively. The peaks in the figure represent different rate-limiting steps detected for the electrode reaction process. P1 and Padd2 observed at high frequency range are related to the anode polarization while P2 and P3 are associated with cathode polarization process[25]. From the figure, the four peaks present different tend with the operation temperature. As can be seen, with the decrease of temperature, P2 and P3 shift to low frequency, while P1 and Padd2 change to high frequency. Moreover, the intensity of P2 and P3 increase significantly compared to that of P1 and Padd2, indicating that the cathode polarization process may be the rate-limiting step at lower temperatures.

Conclusions

LNF and SSC powders were prepared by citric acid combustion and employed as composite cathode for H-SOFCs. LNF-SSC composite material was used as cathode material. The phase structure was characterized by XRD, and it was found that there was good chemical compatibility between LNF cathode and SSC cathode at 1000^oC. The cell with LNF-SSC73 composite cathode displays a higher maximum power density of 636mW cm^{-2} and a lower polarization resistance of 0.10 Ω·cm^2 than that of single-phase LNF cathode and single-phase SSC cathode at 700^oC, indicating that the oxygen reduction reaction in the composite cathode can be significantly accelerated. The above results indicate that LNF-SSC73 can improve the cell electrochemical performance to a certain extent and is a proper cathode material for intermediate-temperature SOFCs with good application prospects.

Declarations

Acknowledgements

This work was supported by the National Natural Science Foundation of China (Grant Nos.: 11875164), Joint Open Fund of Jiangsu Collaborative Innovation Center for Ecological Building Material and Environmental Protection Equipments and Key Laboratory for Advanced Technology in Environmental Protection of Jiangsu Province(Grant No.114269115) and Natural Science Foundation of the Higher Education Institutions of Jiangsu Province (No. 18KJA430017)

References

[1] Bi L, Shafi SP, Da'as EH, Traversa E. Tailoring the Cathode-Electrolyte Interface with Nanoparticles for Boosting the Solid Oxide Fuel Cell Performance of Chemically Stable Proton-Conducting Electrolytes. Small. 2018;14:e1801231.

[2] Lei L, Tao Z, Wang X, Lemmon JP, Chen F. Intermediate-temperature solid oxide electrolysis cells with thin proton-conducting electrolyte and a robust air electrode. Journal of Materials Chemistry A. 2017;5:22945-51.

[3] Ma J, Tao Z, Kou H, Fronzi M, Bi L. Evaluating the effect of Pr-doping on the performance of strontium-doped lanthanum ferrite cathodes for protonic SOFCs. Ceramics International. 2020;46:4000-5.

[4] Bi L, Boulfrad S, Traversa E. Steam electrolysis by solid oxide electrolysis cells (SOECs) with proton-conducting oxides. Chem Soc Rev. 2014;43:8255-70.

[5] Zuo C, Zha S, Liu M, Hatano M, Uchiyama M. Ba(Zr0.1Ce0.7Y0.2)O3−δ as an Electrolyte for Low-Temperature Solid-Oxide Fuel Cells. Advanced Materials. 2006;18:3318-20.

[6] Fabbri E, Pergolesi D, Traversa E. Electrode materials: a challenge for the exploitation of protonic solid oxide fuel cells. Sci. Technol. Adv. Mater. 2010;11: 044301-09..

[7] Fabbri E, Licoccia S, Traversa E, Wachsman ED. Composite Cathodes for Proton Conducting Electrolytes. 2009;9:128-38.

[8] Zhao F, Wang Z, Liu M, Zhang L, Xia C, Chen F. Novel nano-network cathodes for solid oxide fuel cells. Journal of Power Sources. 2008;185:13-8.

[9] Liu W, Kou H, Wang X, Bi L, Zhao XS. Improving the performance of the $Ba_{0.5}Sr_{0.5}Co_{0.8}Fe_{0.2}O_{3-\delta}$ cathode for proton-conducting SOFCs by microwave sintering. Ceramics International. 2019;45:20994-8.

[10] Li G, Zhang Y, Ling Y, He B, Xu J, Zhao L. Probing novel triple phase conducting composite cathode for high performance protonic ceramic fuel cells. International Journal of Hydrogen Energy. 2016;41:5074-83.

[11] Zhao L, Shen J, He B, Chen F, Xia C. Synthesis, characterization and evaluation of $PrBaCo_{2-x}Fe_xO_{5+\delta}$ as cathodes for intermediate-temperature solid oxide fuel cells. International Journal of Hydrogen Energy. 2011;36:3658-65.

[12] Zhu M, Cai Z, Xia T, Li Q, Huo L, Zhao H. Cobalt-free perovskite $BaFe_{0.85}Cu_{0.15}O_{3-\delta}$ cathode material for intermediate-temperature solid oxide fuel cells. International Journal of Hydrogen Energy. 2016;41:4784-91.

[13] Taguchi H, Chiba R, Komatsu T, Orui H, Watanabe K, Hayashi K. LNF SOFC cathodes with active layer using Pr_6O_{11} or Pr-doped CeO_2. Journal of Power Sources. 2013;241:768-75.

[14] Hou J, Qian J, Bi L, Gong Z, Peng R, Liu W. The effect of oxygen transfer mechanism on the cathode performance based on proton-conducting solid oxide fuel cells. Journal of Materials Chemistry A. 2015;3:2207-15.

[15] Tang H, Gong Z, Wu Y, Jin Z, Liu W. Electrochemical performance of nanostructured LNF infiltrated onto LNO cathode for $BaZr_{0.1}Ce_{0.7}Y_{0.2}O_{3-\delta}$–based solid oxide fuel cell. International Journal of Hydrogen Energy. 2018;43:19749-56.

[16] Hou J, Zhu Z, Qian J, Liu W. A new cobalt-free proton-blocking composite cathode $La_2NiO_{4+\delta}$–$LaNi_{0.6}Fe_{0.4}O_{3-\delta}$ for $BaZr_{0.1}Ce_{0.7}Y_{0.2}O_{3-\delta}$–based solid oxide fuel cells. Journal of Power Sources. 2014;264:67-75.

[17] Sun W, Fang S, Yan L, Liu W. Proton-Blocking Composite Cathode for Proton-Conducting Solid Oxide Fuel Cell. Journal of The Electrochemical Society. 2011;158:B1432.

[18] Peng R, Wu T, Liu W, Liu X, Meng G. Cathode processes and materials for solid oxide fuel cells with proton conductors as electrolytes. Journal of Materials Chemistry. 2010;20:6218-25.

[19] Huang B, Zhu X-j, Lv Y, Liu H. High-performance $Gd_{0.2}Ce_{0.8}O_2$-impregnated $LaNi_{0.6}Fe_{0.4}O_{3-\delta}$ cathodes for intermediate temperature solid oxide fuel cell. Journal of Power Sources. 2012;209:209-19.

[20] Tao Z, Bi L, Yan L, Sun W, Zhu Z, Peng R, et al. A novel single phase cathode material for a proton-conducting SOFC. Electrochemistry Communications. 2009;11:688-90.

[21] Lei L, Tao Z, Hong T, Wang X, Chen F. A highly active hybrid catalyst modified $(La_{0.60}Sr_{0.40})_{0.95}Co_{0.20}Fe_{0.80}O_{3-\delta}$ cathode for proton conducting solid oxide fuel cells. Journal of Power Sources. 2018;389:1-7.

[22] Zhao K, Xu Q, Huang D-P, Chen M, Kim B-HJJoSSE. Electrochemical evaluation of $La_2NiO_{4+\delta}$-based composite electrodes screen-printed on $Ce_{0.8}Sm_{0.2}O_{1.9}$ electrolyte. 2012;16:2797-804.

[23] Shi N, Su F, Huan D, Xie Y, Lin J, Tan W, et al. Performance and DRT analysis of P-SOFCs fabricated using new phase inversion combined tape casting technology. Journal of Materials Chemistry A. 2017;5:19664-71.

[24] Zhang Y, Chen Y, Yan M, Chen F. Reconstruction of relaxation time distribution from linear electrochemical impedance spectroscopy. Journal of Power Sources. 2015;283:464-77.

[25] Wang X, Ma Z, Zhang T, Kang J, Ou X, Feng P, et al. Charge-Transfer Modeling and Polarization DRT Analysis of Proton Ceramics Fuel Cells Based on Mixed Conductive Electrolyte with the Modified Anode–Electrolyte Interface. ACS Applied Materials & Interfaces. 2018;10:35047-59.

Figures

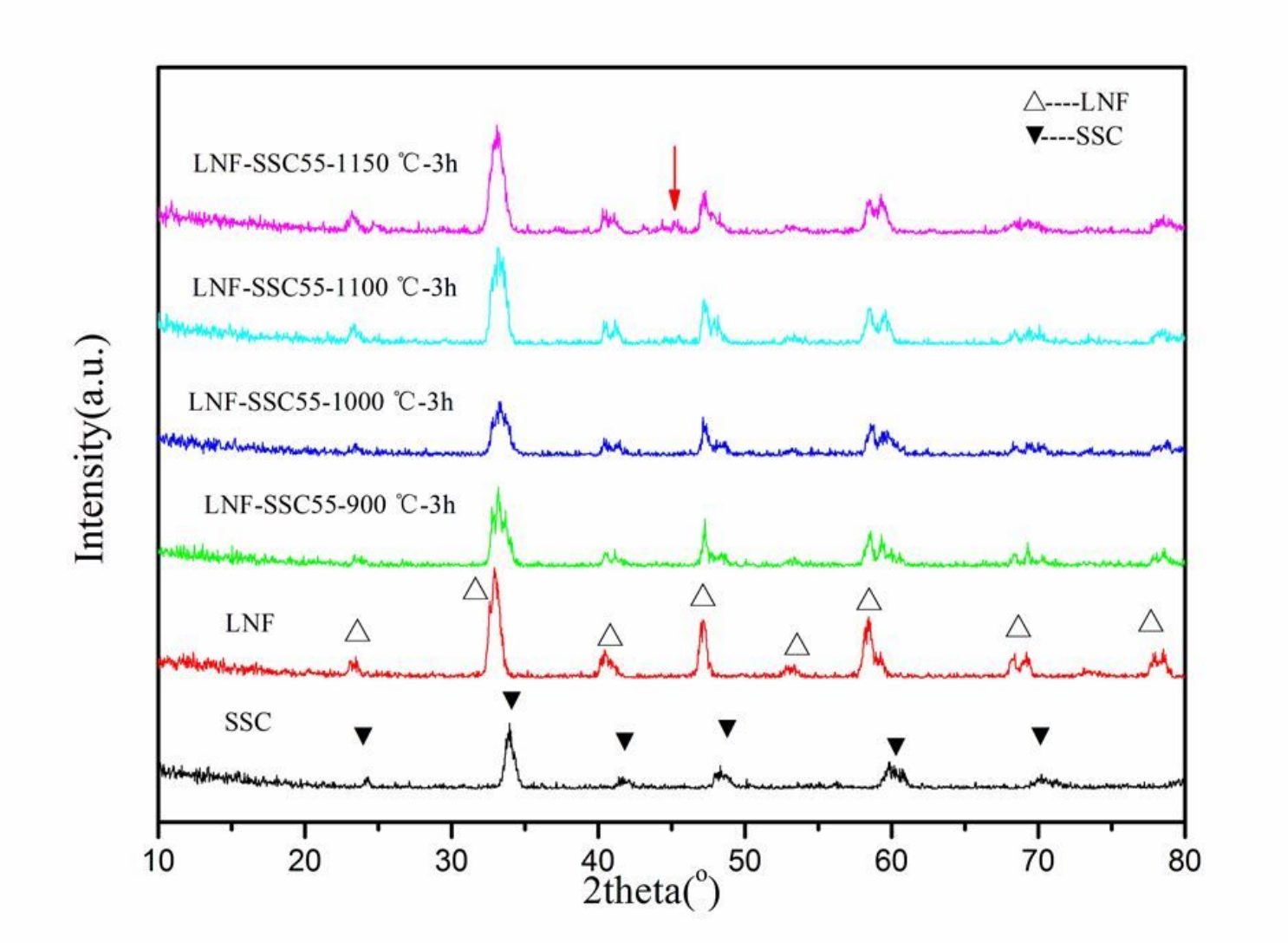

Figure 1

The XRD patterns of as-prepared SSC, LNF and LNF-SSC73 mixtures after co-fired at elevated temperatures for 3h;

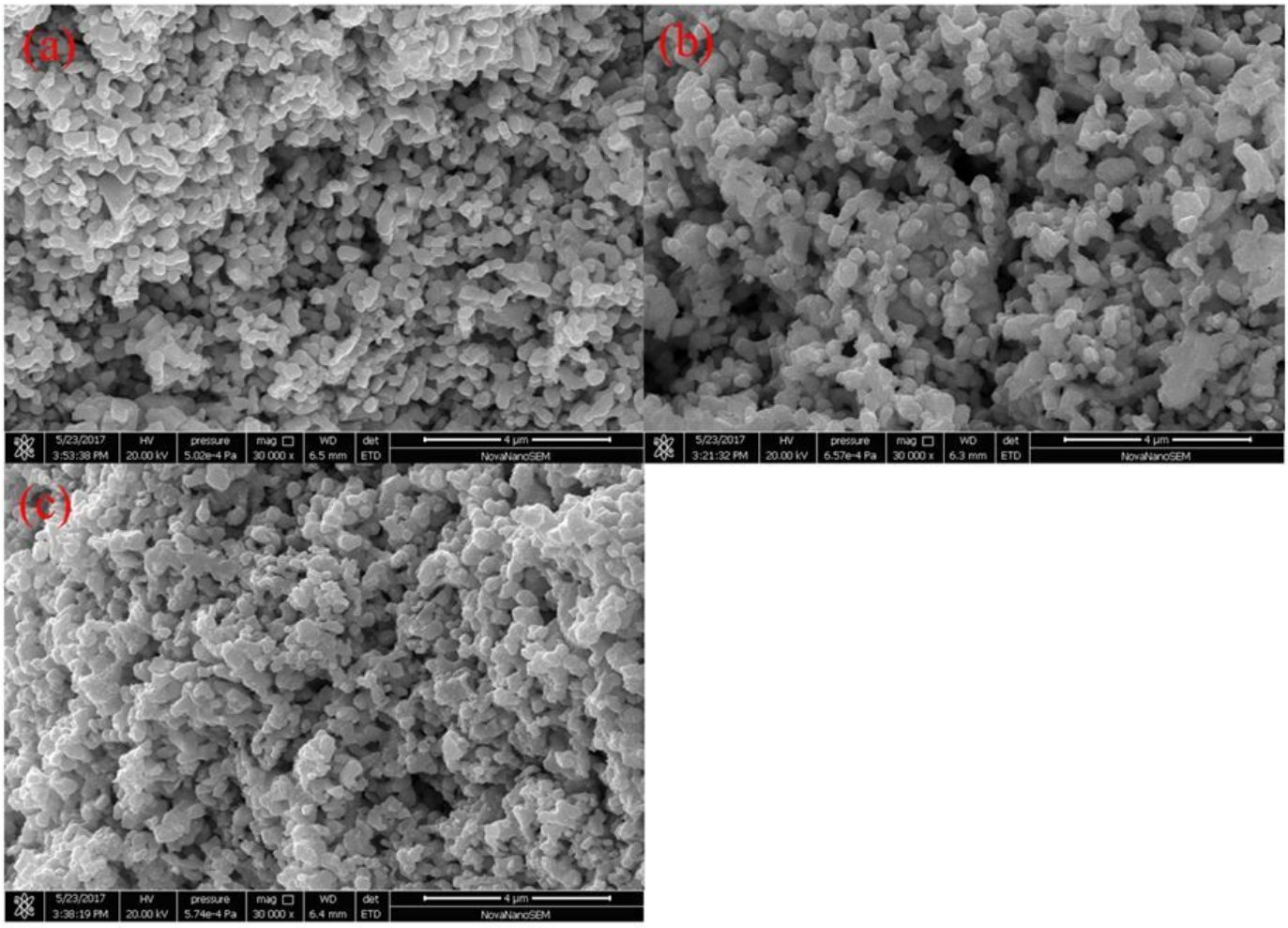

Figure 2

SEM micrographs of the cathode for (a) LNF-SSC10, (b) LNF-SSC01 and (c) LNF-SSC73;

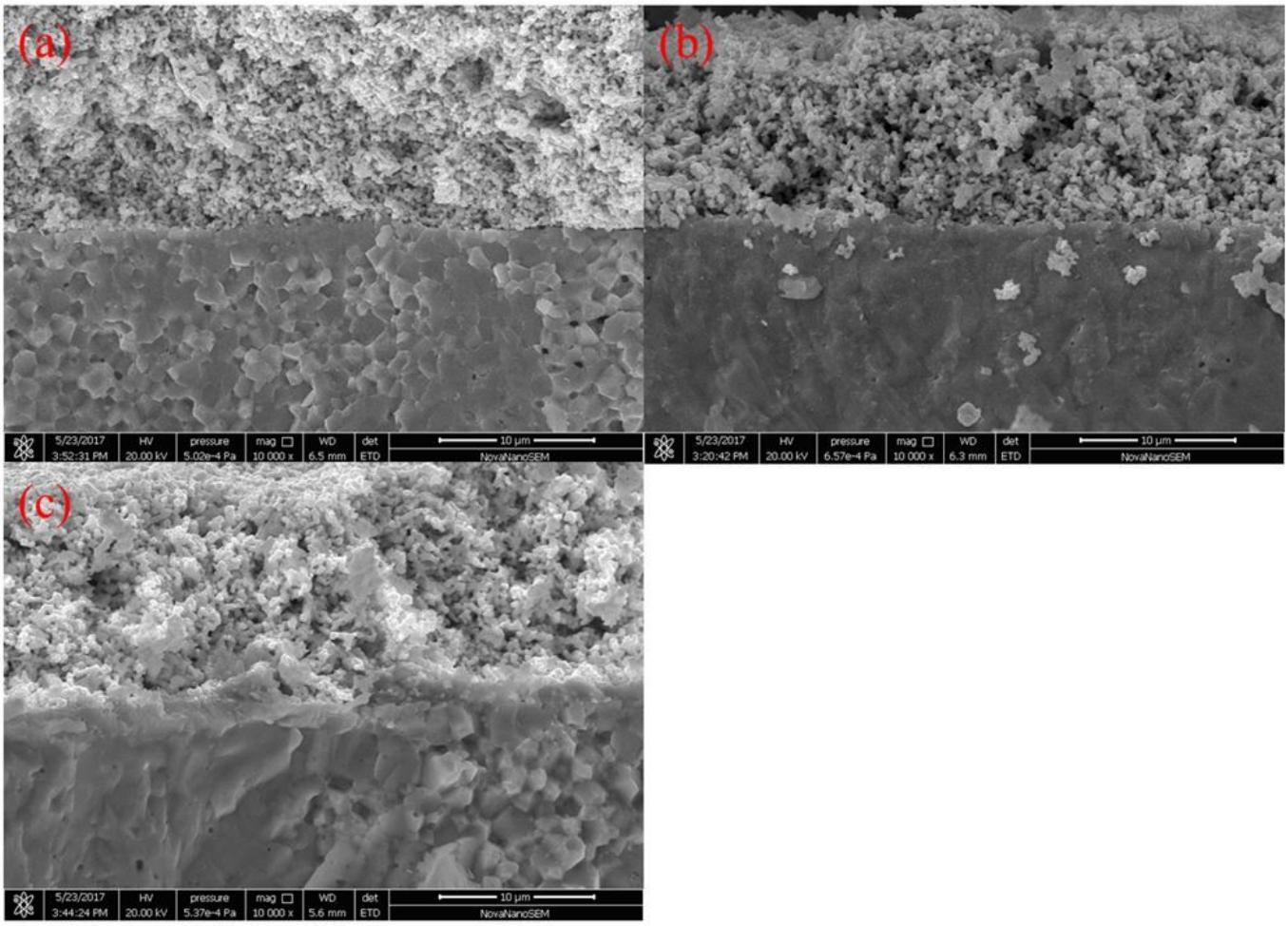

Figure 3

SEM micrographs of the cathode/electrolyte interface for (a) LNF-SSC10, (b) LNF-SSC01 and (c) LNF-SSC73;

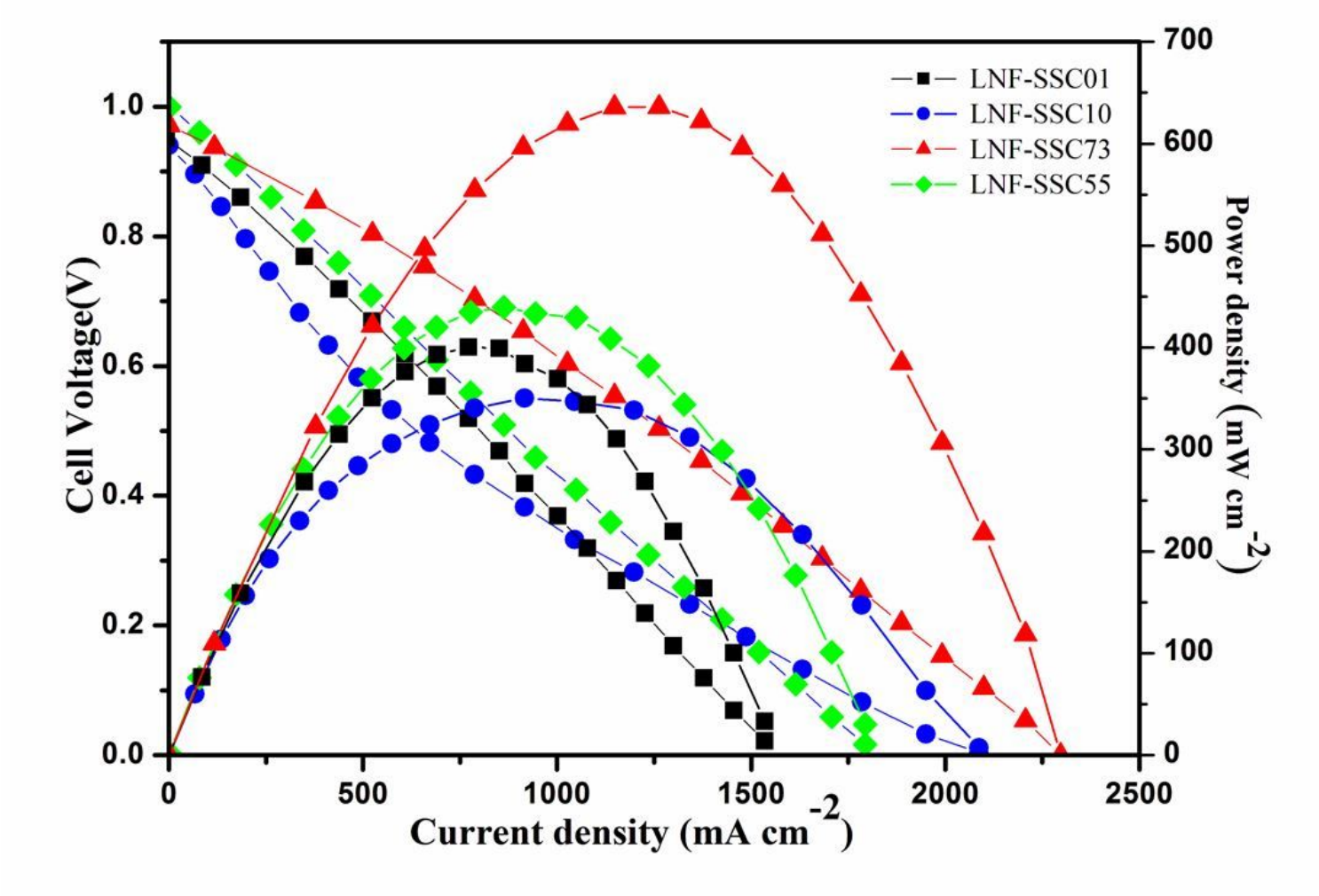

Figure 4

I–V and power density curves for the cell with LNF-SSC composite cathodes measured at 700 °C;

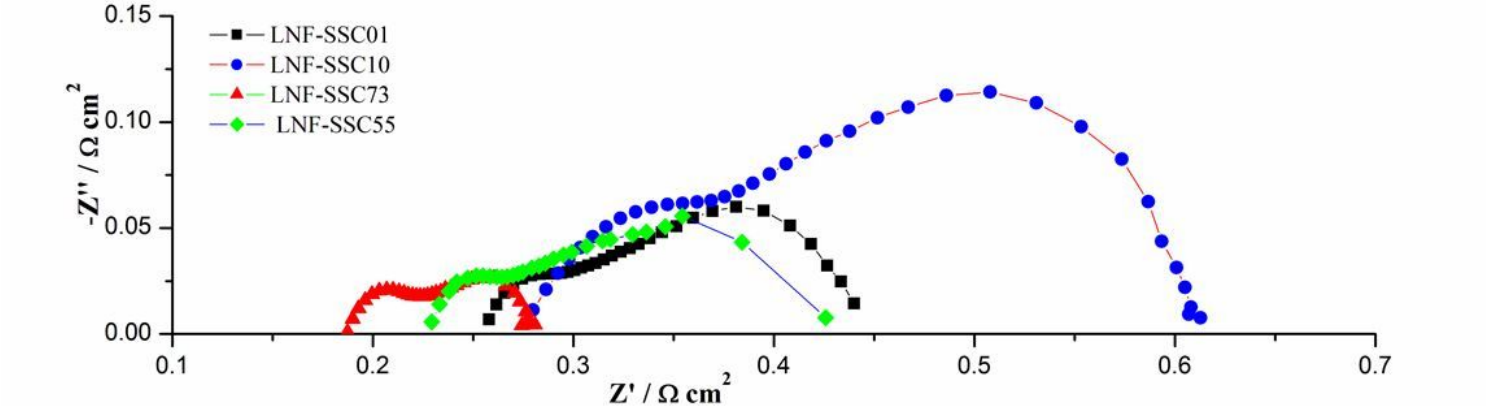

Figure 5

A comparison of impedance plots of fuel cells using LNF-SSC composite cathodes measured at 700 °C;

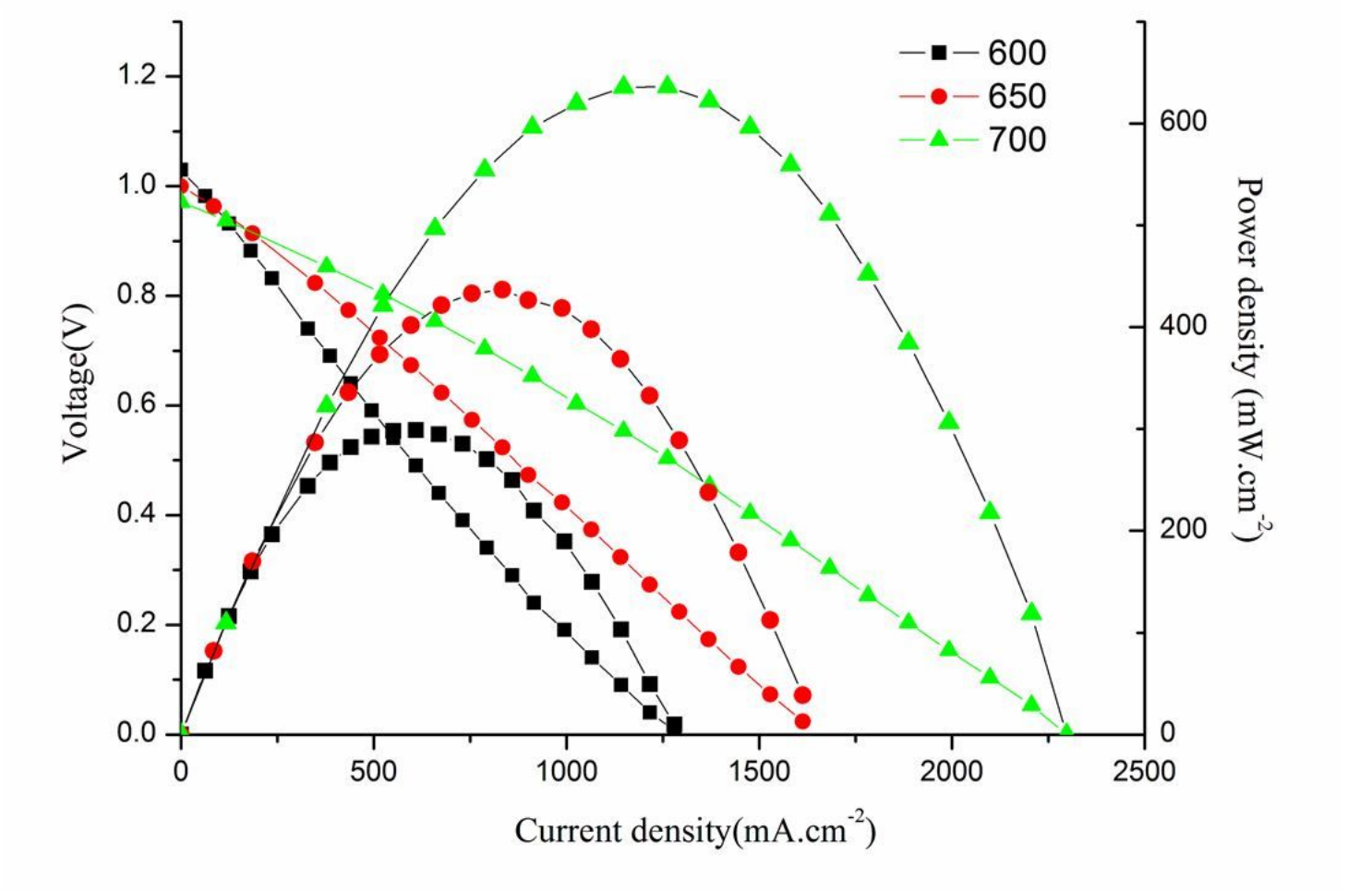

Figure 6

I–V and power density curves for the cell with LNF-SSC73 at 600, 650, and 700 °C;

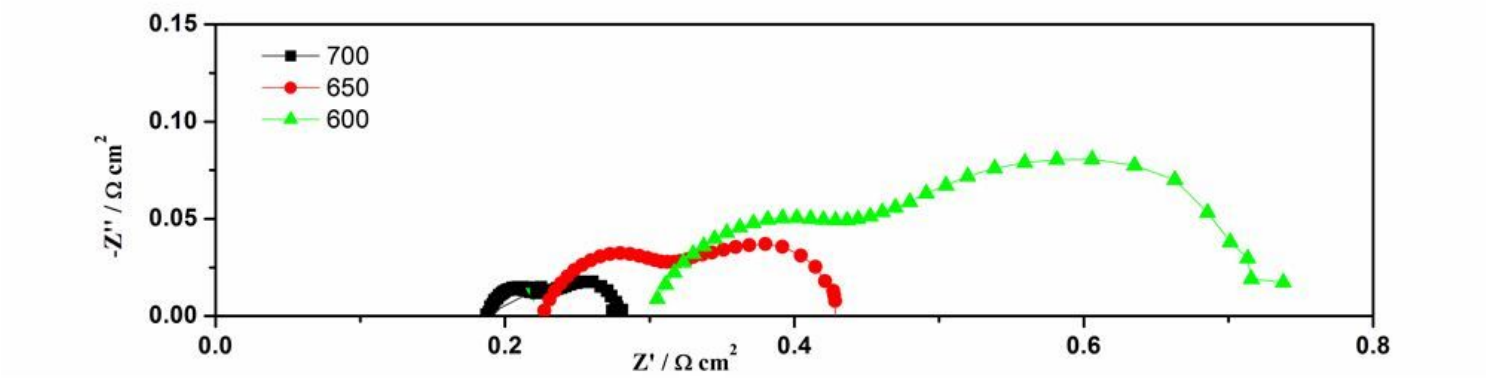

Figure 7

Impedance plots of fuel cells using LNF-SSC73 measured at 600, 650, and 700 °C.

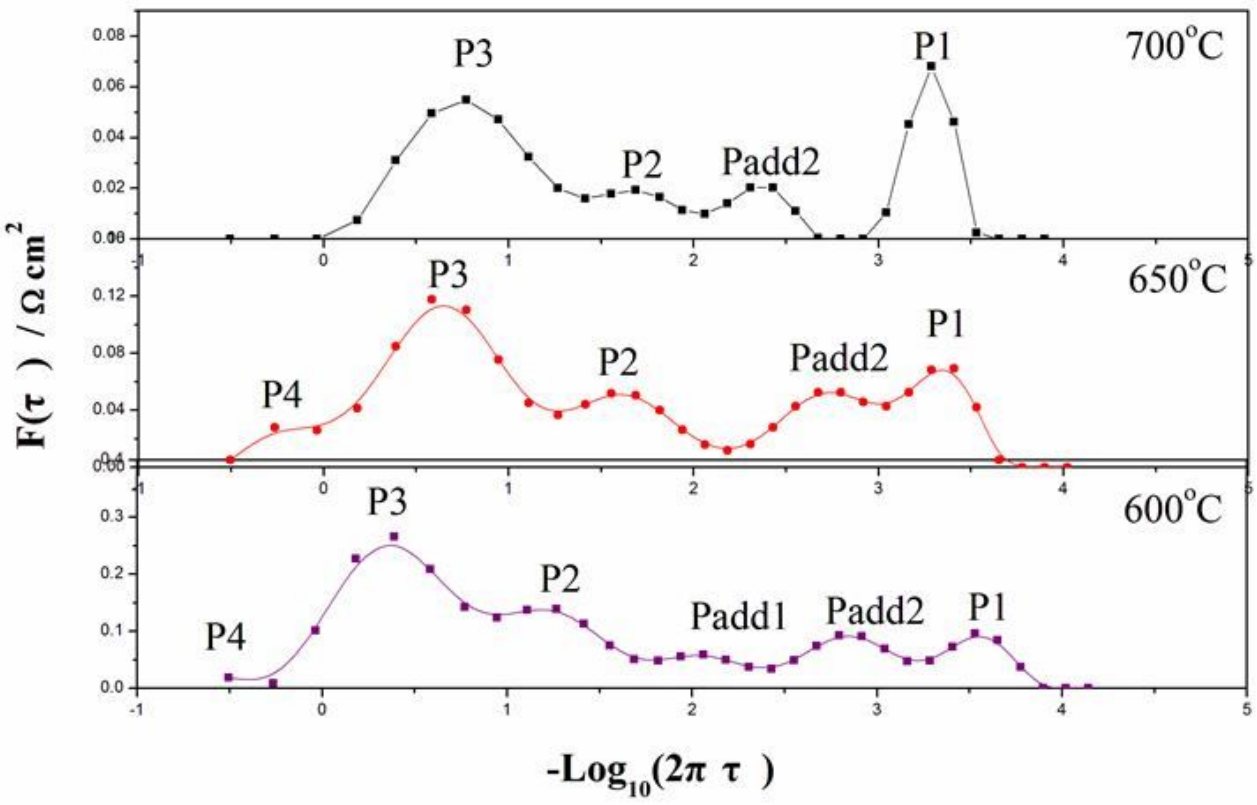

Figure 8

The impedance spectra corresponding distributions of relaxation times plots.